J Nanopart Res (2014) 16:2500
DOI 10.1007/s11051-014-2500-5

BRIEF COMMUNICATION

Fabrication of transparent and flexible Ag three-dimensional mesh electrode by thermal roll-to-roll imprint lithography

Gyutae Kim · Ju-Hyeon Shin · Hak-Jong Choi · Heon Lee

Received: 25 November 2013 / Accepted: 5 June 2014 / Published online: 12 August 2014

Abstract Ag mesh electrode was researched as a replacement for indium–tin oxide electrode in flexible electronics because of its low sheet resistance and high transparency. In this study, Ag mesh pattern created using Ag nanoparticles (20 nm of diameter) was arranged on a patterned polymer substrate using thermal roll-to-roll imprint lithography. Using this method, the Ag mesh-patterned electrode achieved scalability and high throughput. The fabricated Ag 3D mesh electrode showed an average optical transmittance of 69 %, and sheet resistance of 18 Ω/sq was measured for 60 min of annealing time.

Keywords Ag nanoparticle · Flexible and transparent electrode · Metal mesh · Thermal roll to roll

Introduction

Transparent and flexible electrodes are important in many applications such as displays, solar cells, radio-frequency identification chips, circuits, and organic light-emitting diodes (OLEDs) (Forrest 2004; Granqvist 2007; Wu et al. 2008; Zhong et al. 2011). Currently, indium–tin oxide (ITO) is used for transparent conducting films owing to its high transparency (~80 %) in the visible wavelength region and low sheet resistance (10 Ω/sq.). However, ITO has certain problems, such as the fact that it can fracture and crack even at 2–3 % strains of the substrate and its high price because of the gradual depletion of resources (Cairns et al. 2000). For these reasons, ITO is not suitable for future flexible devices. To replace ITO as electrodes, many studies have reported using random arrangements of metal nanowires, graphene films, carbon nanotube films (Guo et al. 2013; Wu et al. 2004; Zhang et al. 2005), poly(3,4-ethylenedioxythiophene): poly(styrenesulfonate) (PEDOT:PSS) polymers (Kirchmeyer and Reuter 2005; MacDiarmid 2001), and metal gratings (Yu et al. 2012). The goal is to fabricate scalable transparent and flexible electrodes using a low-cost manufacturing process. Among the above-mentioned approaches for fabricating transparent and flexible electrodes, the use of metal gratings has several advantages. First, many kinds of metals can be used in order to obtain suitable material properties. Second, metal grating electrodes enable the fabrication of new device structures in OLEDs such as top-emitting devices and tandem structures (Kim et al. 2000; Liu et al. 2005; Ziebarth et al. 2004). Recently, there have been many studies on controlling the electrical, mechanical, and thermal properties of nanomaterials (Krebs 2009; Espinosa et al. 2011; Krebs et al. 2007;

G. Kim · J.-H. Shin · H.-J. Choi · H. Lee (✉)
Department of Materials Science and Engineering, Korea University, Anam-dong 5-ga, Seongbuk-gu, Seoul 136-713, South Korea
e-mail: heonlee@korea.ac.kr

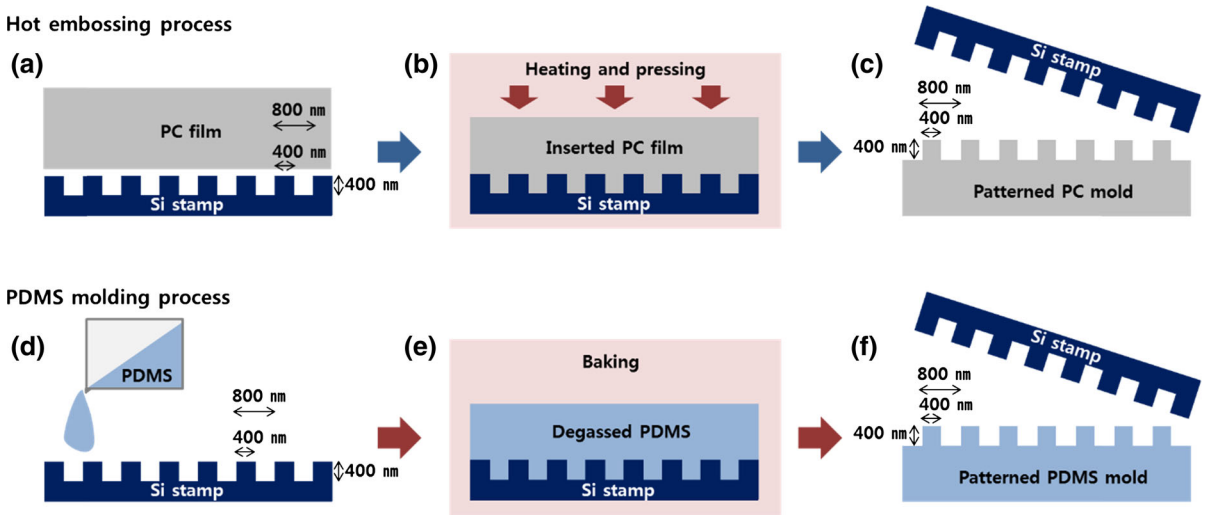

Fig. 1 Schematic diagram showing the hot-embossing process: **a** Dimensions of Si master stamp, **b** heating and pressing process, and **c** replicated patterned PC mold. Schematic diagram showing PDMS molding process: **d** Pouring PDMS onto Si stamp, **e** baking process, and **f** dimensions of replicated patterned PDMS mold

Ahn et al. 2009; Lee et al. 2012; Zhang et al. 2012; MacCuspie 2011). The small sizes of these nanomaterials make it possible to use solution processes to form variously shaped structures or sheets. Thermal roll-to-roll imprint lithography is a suitable solution process because it does not require the use of vacuum and high temperatures.

We demonstrate here that thermal roll-to-roll imprint lithography is suitable for fabricating transparent and flexible Ag three-dimensional (3D) mesh electrodes.

Experimental details

Fabrication of patterned polymer substrate

The transparent and flexible Ag 3D mesh electrode consisted of the following layers: inserted lower Ag lines in patterned polycarbonate (PC) and aligned upper Ag lines. A Si master stamp with 400 nm of height, line and space width was used to fabricate this 3D mesh electrode. The Si master stamp (50×50 mm^2) was coated with a self-assembled monolayer (SAM) for easy detachment of the polymer from the Si master stamp. Heptadecafluoro-1,1,2,2-tetra-hydrodecyl and n-hexane were used for the SAM coating for the liquid-phase self-assembly process (Jung et al. 2004).

In this study, a patterned PC substrate of the electrode was used for the flexible transparent electrode. The substrate was fabricated by a hot-embossing process, which facilitates high-fidelity 1:1 scale replication with low cost. The non-patterned PC film, with a glass transition temperature (T_g) of 147 °C, was placed on the Si master stamp (Fig. 1a), and the substrate was held at 200 °C for 20 min (Fig. 1b). Subsequently, 20 bar (2 MPa) of air pressure was applied for 20 min to form the pattern on the PC substrate. After the heating and pressing process, the patterned PC substrate was detached from the Si master stamp (Fig. 1c). For the upper vertically aligned Ag lines for the 3D mesh electrode, a patterned polydimethylsiloxane (PDMS) mold was used (Fig. 1d–f). Because of the different surface energies between the PC film and the PDMS, the Ag nanoparticle ink was attached on the PC film after thermal roll-to-roll imprint lithography. PDMS enabled the conformal contact to substrate without surface flatness of the substrate. The patterned PDMS mold was duplicated from the Si master stamp using a thermal-hardening process.

Thermal roll-to-roll imprint lithography

Thermal roll-to-roll imprint lithography (CMP Co., Ltd.) was adopted because it enables control of the layer thickness by using an appropriate volume of Ag

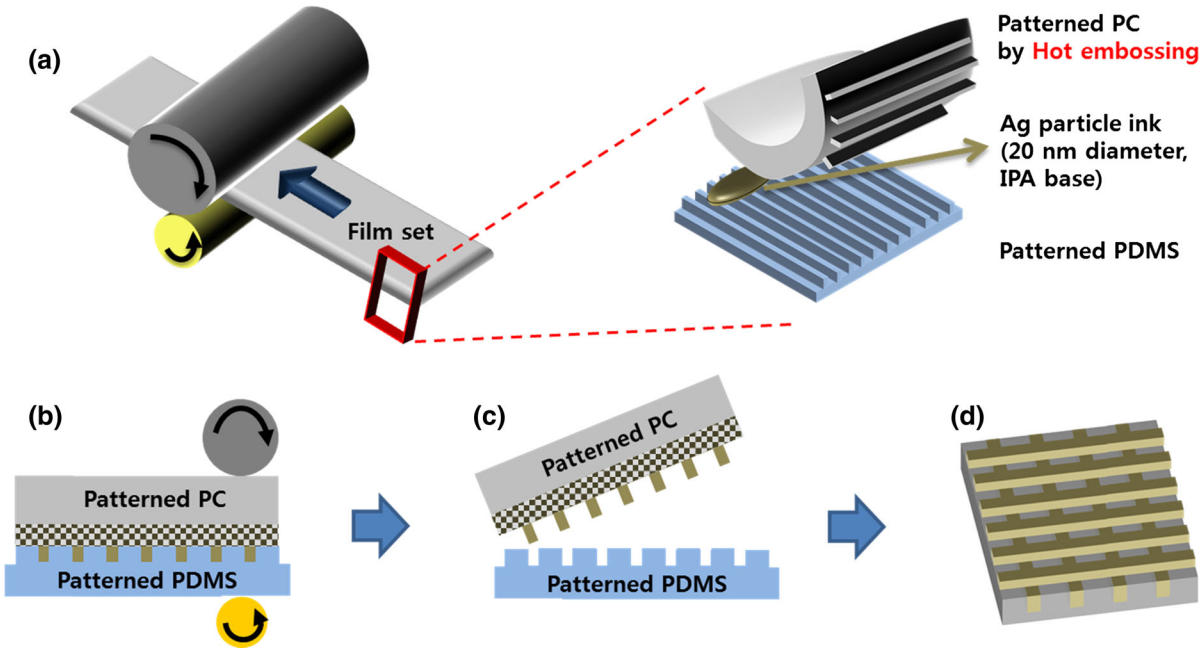

Fig. 2 Schematic diagram showing the fabrication of a 3D Ag mesh electrode: **a** Film set of Ag nanoparticle ink, patterned PC, and PDMS mold. **b** Thermal roll-to-roll imprint lithography process. **c** Detaching patterned PC substrate from the patterned PDMS. **d** Tilted schematic diagram of 3D Ag mesh transparent flexible electrode

nanoparticle ink and by controlling the roll speed, operation temperature, and pressure. A 20-nm Ag nanoparticle ink (DGP 40LT-15C, Advanced Nano Products Co., Ltd.) was found to be suitable for fabricating 3D mesh electrodes with 400-nm-sized lines. The isopropyl alcohol (IPA)-based Ag ink had a solid content of 35 % and a viscosity of 15 cPS (15 mPa s). The patterned PC substrate served as the flexible electrode, the Ag nanoparticle ink was used as the electrode material, and the patterned PDMS functioned as the upper electrode lines. The Ag nanoparticle ink was dropped onto the patterned PDMS mold by 20 $\mu l/cm^2$, and then another patterned PC mold is placed on top of and perpendicular to the Ag nanoparticle ink/patterned PDMS mold (Fig. 2a). This film set was inserted between the rollers at a temperature of 100 °C, a pressure of 5 bar (0.5 MPa), and a rate of 5 mm/s. (Figure 2b–d).

Electrode characterization

The morphology of the Ag 3D mesh pattern was determined by FE-SEM (EX-200, Horiba Inc.). The optical transmittance and sheet resistance were measured through a UV–Visible spectrometer (V650 Spectrophotometer, Jasco Inc.) and a 4-point probe resistivity mapping instrument (CMT-SERIES, Advanced Instrument Technology Inc.), respectively.

Results and discussion

Figure 3 shows the FE-SEM images of the fabricated Ag 3D mesh electrode using the proposed one-step thermal roll-to-roll imprint lithography process. This one-step process of fabricating 3D structures has the advantage of high throughput compared to two-step nanoimprint lithography previously reported (Kang and Guo 2007). The 300 nm-sized Ag 3D mesh pattern was fabricated on the patterned PC substrate over the whole substrate area (50 × 50 mm^2). In the patterned area, which is the bright color in Fig. 3a, the line width was reduced to 300 nm. This reduction of line width comes from the absorption of the solvent and the thermal shrinkage that occurs during the thermal roll-to-roll imprint lithography and annealing processes. In the non-patterned area, which is the dark color in Fig. 3a, the surface of the PC substrate

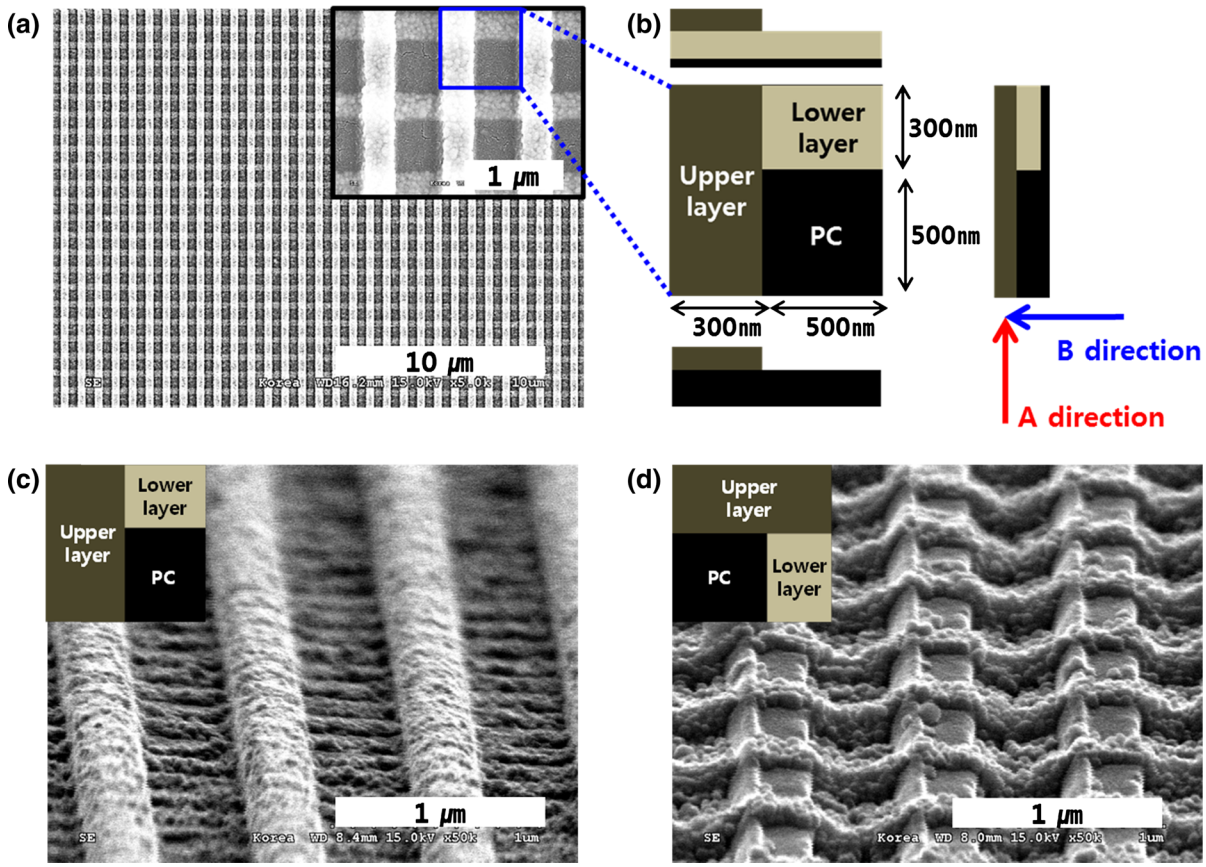

Fig. 3 FE-SEM image of Ag 3D mesh electrode: **a** *Top view* (*inset*: high magnification). **b** Illustration of unit cell, **c** A-direction *tilted view* of the Ag 3D mesh electrode, and **d** B-direction *tilted view* of the Ag 3D mesh electrode

without a residual layer of Ag nanoparticles is visible, which causes problems in electronic devices. This non-residual layer of Ag nanoparticles is the result of the thermal roll-to-roll imprint lithography, where residual Ag ink during formation of the upper layer is put down to lower layer which was made up of empty space area. The unit cell diagram of the Ag 3D mesh electrode is shown in Fig. 3b, which also shows the cross-sections of the electrode in directions A and B. The upper layer of Ag lines is placed perpendicular to the lower layer of Ag lines. Figure 3c, d show tilted SEM images in the A- and B-direction, respectively. This upper layer, which is connected to the lower layer, distributes the current flow in the Ag 3D mesh electrodes. The thickness of the upper layer is about 50–100 nm, which is the diameter of one or two Ag nanoparticles after annealing.

For transparent and flexible electrodes, the optical transmittance and sheet resistance are important

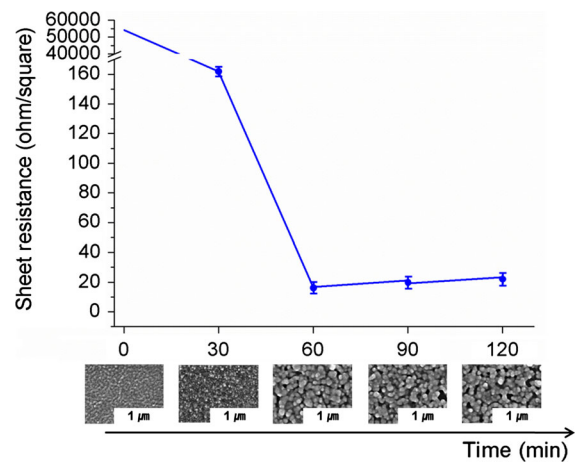

Fig. 4 Sheet resistance of Ag 3D mesh electrode as a function of annealing time

properties. Higher the optical transmittance of the electrode, higher its sheet resistance. In Fig. 4, the sheet resistance of the Ag 3D mesh electrode is shown

as a function of annealing time. The annealing process is necessary in order to remove solvent residue such as the dispersant. To minimize deformation of the PC substrate, which has a glass transition temperature (T_g) of 147 °C, the annealing process was carried out at 120 °C. The bottom SEM images indicate characteristic morphological changes of the Ag nanoparticles as a function of annealing time. Until reaching an annealing time of 60 min, the Ag nanoparticles agglomerated with other Ag nanoparticles, showing diameters of 50–100 nm as the annealing time increased. These agglomerated Ag nanoparticles decreased the number of grain boundaries, resulting in an increased electron flow. After 60 min, there was no additional change in diameter, but there were more disconnected areas. The initial Ag 3D mesh electrode exhibited 55,000 Ω/sq. of sheet resistance, but it decreased to 160 Ω/sq. after 30 min of annealing time, during which time most of the residue was removed. Thus, the Ag nanoparticle was connected to each other with no surrounding material. The lowest sheet resistance of 18 Ω/sq. was measured after 60 min of annealing time. Electrodes annealed for more than 60 min were shown to have higher sheet resistance as compared with the sample annealed for 60 min due to its greater number of disconnected areas. Consequently, we chose to use 60 min of annealing time to measure the optical transmittance.

In Fig. 5a, the optical transmittance of the reference PC, the Ag 3D mesh electrode, and the Ag nanoparticles coated on PC are shown. The Ag nanoparticles coated on PC were fabricated using blanket PDMS and a PC substrate patterned with 400 nm lines by thermal roll-to-roll imprint lithography under the same conditions used to fabricate the Ag 3D mesh electrode. We increased the optical transmittance by fabricating the 3D mesh structure. The Ag 3D mesh electrode showed an average optical transmittance of 69 %, whereas for the Ag nanoparticles coated on PC, the average optical transmittance was only 30 %. An absorption peak at approximately 300 nm resulted from the line pattern of the patterned PC. As shown in Fig. 5b, the Ag 3D mesh electrode shows better transmittance than the Ag nanoparticles coated on PC.

Thus, an Ag 3D mesh structure with good electrical properties can be made from the Ag ink that is widely used in printed electronics. Without needing a vacuum deposition process, this manufacturing technique enables the fabrication for transparent and flexible devices.

Conclusion

We have presented a low cost, high-throughput procedure for the fabrication of transparent and flexible silver electrodes on a submicron scale. The fabricated Ag 3D mesh structured electrode shows high optical transmittance in the visible wavelength range and excellent electrical conductivity. Using this method, it is possible to fabricate electrodes for many applications such as organic and wearable devices.

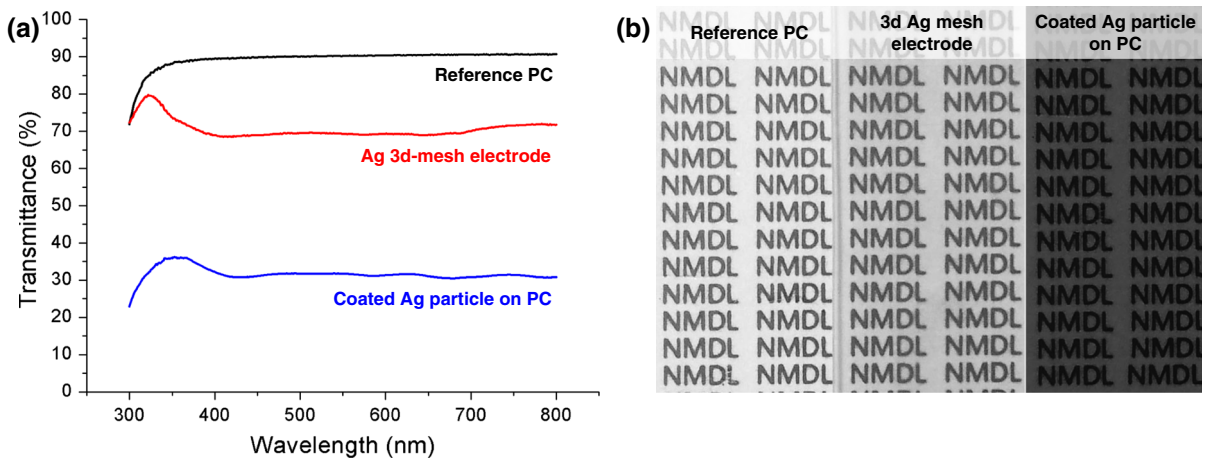

Fig. 5 **a** Optical transmittance of the reference PC, Ag 3D mesh electrode, and Ag nanoparticles coated on PC. **b** Photograph of transmittance comparison of the reference PC, Ag 3D mesh electrode, and Ag nanoparticles coated on PC

References

Ahn BY, Duoss EB, Motala MJ, Guo X, Park S, Xiong Y, Yoon J, Nuzzo RG, Rogers JA, Lewis JA (2009) Omnidirectional printing of flexible, stretchable, and spanning silver microelectrodes. Science 323:1590–1593

Cairns DR, Witte RP, Sparacin DK, Sachsman SM, Paine DC, Crawford GP, Newton RR (2000) Strain-dependent electrical resistance of tin-doped indium oxide on polymer substrates. Appl Phys Lett 76:1425

Espinosa N, Garcia-Valverde R, Urbina A, Krebs FC (2011) Roll-to-roll fabrication of polymer solar cells. A life cycle analysis of polymer solar cell modules prepared using roll-to-roll methods under ambient conditions. Sol Energy Mater Sol Cells 95:1293–1302

Forrest SR (2004) The path to ubiquitous and low-cost organic electronic appliances on plastic. Nature 428:911–918

Granqvist CG (2007) Transparent conductors as solar energy materials: a panoramic review. Sol Energy Mater Sol Cells 91:1529–1598

Guo H, Lin N, Chen Y, Wang Z, Xie Q, Zheng T, Gao N, Li S, Kang J, Cai D, Peng D-L (2013) Copper nanowires as fully transparent conductive electrodes. Sci Rep 3:2323

Jung GY, Ganapathiappan S, Li X, Ohlberg DAA, Olynick DL, Chen Y, Tong WM, Wiliams RS (2004) Fabrication of molecular-electronic circuits by nanoimprint lithography at low temperatures and pressures. Appl Phys A 78:1169–1173

Kang MG, Guo LJ (2007) Nanoimprinted semitransparent metal electrodes and their application in organic light-emitting diodes. Adv Mater 19:1391–1396

Kim JS, Ho PKH, Greenham NC, Friend RH (2000) Electroluminescence emission pattern of organic light-emitting diodes: implications for device efficiency calculations. J Appl Phys 88:1073

Kirchmeyer S, Reuter K (2005) Scientific importance, properties and growing applications of poly(3,4-ethylenedioxythiophene). J Mater Chem 15:2077–2088

Krebs FC (2009) Fabrication and processing of polymer solar cells: a review of printing and coating techniques. Sol Energy Mater Sol Cells 93:394–412

Krebs FC, Spanggaard H, Kjaer T, Biancardo M, Alstrup J (2007) Large area plastic solar cell modules. Mater Sci Eng 138:106–111

Lee P, Lee J, Lee H, Yeo J, Hong S, Nam KH, Lee D, Lee SS, Hwan SH (2012) Highly stretchable and highly conductive metal electrode by very long metal nanowire percolation network. Adv Mater 24:3326–3332

Liu C, Kamaev V, Vardeny ZV (2005) Efficiency enhancement of an organic light-emitting diode with a cathode forming two-dimensional periodic hole array. Appl Phys Lett 86:143501

MacCuspie RI (2011) Colloidal stability of silver nanoparticles in biologically relevant conditions. J Nanopart Res 13:2893–2908

MacDiarmid AG (2001) Synthetic metals: a novel role for organic polymers (nobel lecture). Angew Chem Int Ed 40:2581–2590

Wu Z, Chen Z, Du X, Logan JM, Sippel J, Nikolou M, Kamaras K, Reynolds JR, Tanner DB, Hebard AF, Rinzler AG (2004) Transparent, conductive carbon nanotube films. Science 305:1273–1276

Wu J, Becerril HA, Bao Z, Liu Z, Chen Y, Peumans P (2008) Organic solar cells with solution-processed graphene transparent electrodes. Appl Phys Lett 92:263302

Yu J-S, Kim L, Kim J-S, Jo J, Larsen-Olsen TT, Søndergaard RR, Hösel M, Angmo D, Jørgensen M, Krebs FC (2012) Silver front electrode grids for ITO-free all printed polymer solar cells with embedded and raised topographies, prepared by thermal imprint, flexographic and inkjet roll-to-roll processes. Nanoscale 4:6032–6040

Zhang M, Fang S, Zakhidov AA, Lee SB, Aliev AE, Wiliams CD, Atkinson KR, Baughman RH (2005) Strong, transparent, multifunctional carbon nanotube sheets. Science 309:1215–1219

Zhang L, Liu H, Zhao Y, Sun X, Wen Y, Guo Y, Gao X, Di C, Yu G, Liu Y (2012) Inkjet printing high-resolution, large-area graphene patterns by coffee-ring lithography. Adv Mater 24:436–440

Zhong C, Duan C, Huang F, Wu HB, Cao Y (2011) Materials and devices toward fully solution processable organic light-emitting diodes. Chem Mater 23:326–340

Ziebarth JM, Saafir AK, Fan S, McGehee MD (2004) Extracting light from polymer light-emitting diodes using stamped bragg gratings. Adv Funct Mater 14:451–456